

# Effect of magnetic field annealing on the giant magnetoimpedance in FeCuMoSiB ribbons

Wanjun Ku, Fuding Ge, and Jing Zhu<sup>a)</sup>

Central Iron and Steel Research Institute, Beijing 100081, People's Republic of China

(Received 11 October 1996; accepted for publication 3 July 1997)

The magnetic permeability and giant magnetoimpedance effect of Fe<sub>73.5</sub>Cu<sub>1</sub>Mo<sub>3</sub>Si<sub>13.5</sub>B<sub>9</sub> alloy ribbons in different annealed states have been measured as functions of the external magnetic field and the ac driving current frequency. It is found that the giant magnetoimpedance effect in the magnetic-field annealed state is larger than that in the nonfield annealed state. In the field annealed state, the easy magnetization direction is along the driving current as well as the external magnetic field. This leads to significant change of the permeability at high frequencies, and consequently the magnetoimpedance is enhanced in this state. © 1997 American Institute of Physics. [S0021-8979(97)03420-8]

## I. INTRODUCTION

Recently, many authors have reported on sensitive magnetoinductive and giant magnetoimpedance effects in CoFeSiB amorphous wires (ribbons)<sup>1-4</sup> and FeCuNbSiB alloy wires (films).<sup>5,6</sup> These effects can be explained with the classical electromagnetic theory. Both CoFeSiB amorphous wires (ribbons) and FeCuNbSiB wires (films) show excellent soft magnetic properties.<sup>4,7</sup> When a dc external magnetic field ( $H_{ex}$ ) is applied along the samples, the transverse magnetic flux originated from the ac driving current ( $I_{ac}$ ) is suppressed, thus the transverse magnetic permeability ( $\mu_m$ ) decreases and the magnetic penetration depth ( $\delta$ ) increases. As a result, the ribbon subjected to  $H_{ex}$  exhibits a lower value of impedance ( $Z=R+iX$ ) than that subjected to zero-external magnetic field.<sup>8</sup>

After annealed at the optimum temperature, FeCuMoSiB alloy ribbons show superior soft magnetic properties due to the formation of a homogeneous ultrafine bcc-FeSi grain structure with grain size of several tens nanometer embedded in the residual amorphous matrix.<sup>7,9</sup> We had obtained the relations between giant magnetoimpedance (GMI) and the soft magnetic properties of Fe<sub>73.5</sub>Cu<sub>1</sub>Mo<sub>3</sub>Si<sub>13.5</sub>B<sub>9</sub> alloy ribbons: after the specimen annealed at 793 K for 1 h, it showed both the maximum GMI and excellent soft magnetic properties.<sup>10</sup>

With regard to the magnetic response of the impedance, Panina and Mohri<sup>8</sup> pointed out two principal cases: the easy magnetization direction, which is also the orientation of magnetic domain, is perpendicular or parallel to  $I_{ac}$ . Though the first case has been discussed extensively,<sup>1-4,6,8,11,12</sup> there are only a few articles based on the second case.<sup>8,13-15</sup>

In this article, we present some results of GMI effects in Fe<sub>73.5</sub>Cu<sub>1</sub>Mo<sub>3</sub>Si<sub>13.5</sub>B<sub>9</sub> alloy ribbons in the second case, that is, the easy magnetization direction of the sample is along  $I_{ac}$ , and this was achieved by thermal annealing the sample at 793 K with a dc magnetic field ( $H_a$ ).

## II. EXPERIMENTAL PROCEDURE

The FeCuMoSiB alloy ribbons were prepared by single roller rapidly quenching method. The width and thickness of these ribbons are 20 mm and 25  $\mu$ m, respectively. In order to measure GMI effects in the second case, the experimental arrangements were designed as shown in Fig. 1:  $x$  and  $y$  were the transverse and longitudinal directions of the ribbon,  $z$  was along the ribbon thickness.

To measure the complex impedance, some rectangular samples were cut from the ribbons into pieces with 20 mm along  $x$  and 3 mm along  $y$  before the ribbons were annealed. The ribbons were then wound into cores with 20.2 mm i.d. and 20.6 mm o.d. for measuring the dc  $B-H$  curves and permeability. Then, both the rectangular samples and cores were annealed at 793 K for 1 h, with the application of a magnetic field of 24 KA/m ( $H_a$ ) along  $x$ , and  $H_a$  would introduce an easy magnetization direction. When measuring impedance, a 10 mA of ac driving current ( $I_{ac}$ ) was adopted with the application of an external magnetic field ( $H_{ex}$ ) along  $x$ .  $H_{ex}$  was applied by a solenoid. In such way, the easy magnetization,  $H_{ex}$  and  $I_{ac}$  were all in the same direction, therefore GMI in the second case was achieved.

Using the four-terminal measurement method and an impedance analyzer (HP4192A), the magnetic permeability (under a magnetic field of 0.156 A/m) and impedance were measured. The dc  $B-H$  curves were measured with an automatic hysteresis loop tracer. Here, we define GMI( $R, X, Z$ ) as

$$\text{GMI}(R, X, Z) = \frac{R, X, Z_{(H_{ex})} - R, X, Z_{(H_{ex}=0)}}{R, X, Z_{(H_{ex}=0)}} \times 100\% \quad (1)$$

$$Z = R + iX.$$

## III. RESULTS AND DISCUSSION

Figure 2 shows the dc  $B-H$  curves of the field and non-field annealed samples. As shown in this figure, different types of  $B-H$  curves could be obtained by different thermal annealing. In the field annealed state, the easy magnetization was along the transverse direction of the ribbons and this led to a flat  $B-H$  curve.

<sup>a)</sup>Also with Department of Materials Science and Engineering, Tsinghua University, Beijing 100084, People's Republic of China.

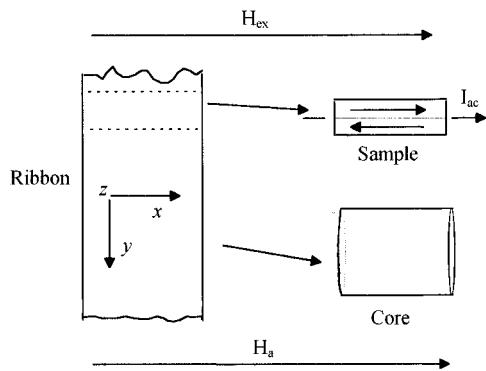


FIG. 1. Schematic arrangements for thermal annealing with magnetic field ( $H_a$ ) and for measuring magnetic properties under the external magnetic field ( $H_{ex}$ ). The orientation of magnetic domain representing the easy magnetization direction and the ac driving current ( $I_{ac}$ ) are also shown.

Figures 3(a) and 3(b) show the frequency dependence of the permeability. It is obvious that the permeabilities decreased to very low values when  $H_{ex}$  was applied. It also can be seen that the relaxation frequency ( $\omega_\tau$ ) moved from 100 to 200 kHz in the field annealed state while from 30 to 70 kHz in the nonfield annealed state. In order to clarify the magnetic properties,  $\Delta\mu/\mu_{(H_{ex}=0)}$  ( $\Delta\mu = \mu_{(H_{ex})} - \mu_{(H_{ex}=0)}$ ,  $\mu = \mu' + i\mu''$ ) of the two states are shown in Fig. 4. Here,  $\mu'$  and  $\mu''$  are the real and imaginary parts of the permeability, respectively. Figure 4 clearly shows that with the increase of frequency,  $\Delta\mu/\mu_{(H_{ex}=0)}$  decreased in both states, but in the field annealed state it was larger and decreased more slowly than that in the nonfield annealed state. This phenomena is associated with the different transverse magnetization process in the two states. It is well known that the magnetization is proceeded by both domain wall movement and magnetic moment rotation, the former characterized by a relaxation frequency  $\omega_{ds}$  and the latter by  $\omega_{rot}$ , and generally  $\omega_{ds} < \omega_{rot}$ . Since the susceptibility is very high, the magnetic permeability can be written as

$$\mu = \frac{\mu^0}{1 - i \frac{\omega}{\omega_\tau}} \quad (2)$$

Here,  $\mu^0$  is the static permeability,  $\omega$  is the ac driving current frequency, and  $\omega_\tau$  represents either  $\omega_{ds}$  or  $\omega_{rot}$ .

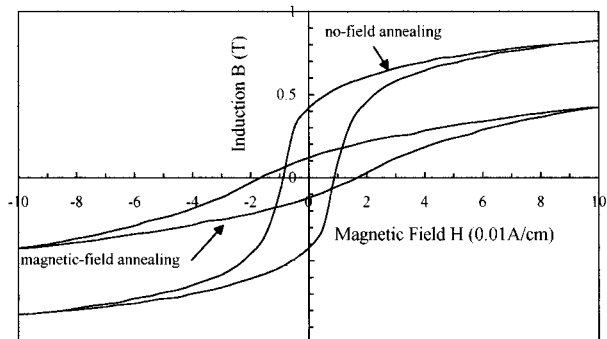


FIG. 2. dc  $B-H$  curves of  $Fe_{73.5}Cu_1Mo_3Si_{13.5}B_9$  alloy ribbons in magnetic- and nonfield annealed states.

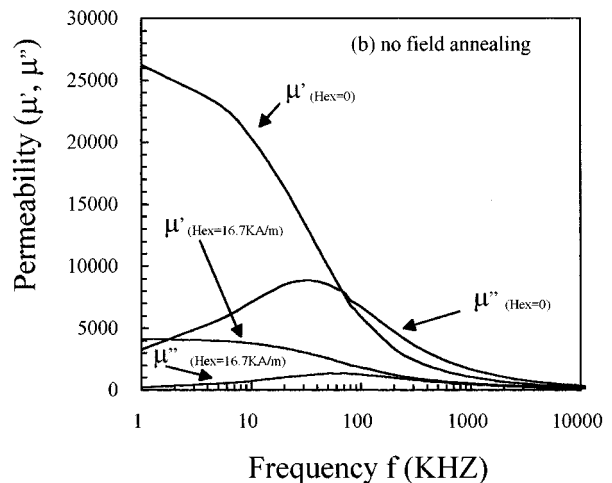
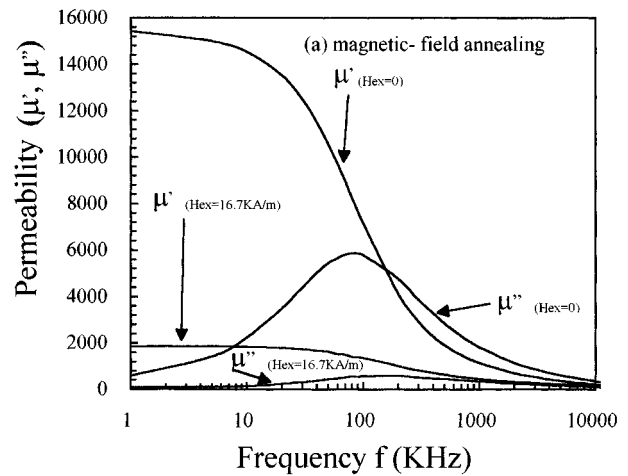


FIG. 3. Frequency dependence of permeability ( $\mu$ ) in (a) magnetic-field and (b) nonfield annealed states.  $\mu = \mu' + i\mu''$ ,  $\mu'$  and  $\mu''$  represents the real and imaginary parts of the permeability, respectively.

In the field annealed state, the moment rotation dominated the magnetization process. This resulted in a larger relaxation frequency, a lower magnetic permeability, and a slow decrease of the permeability with the increase of frequency. When  $H_{ex}$  was applied, the domains were along the

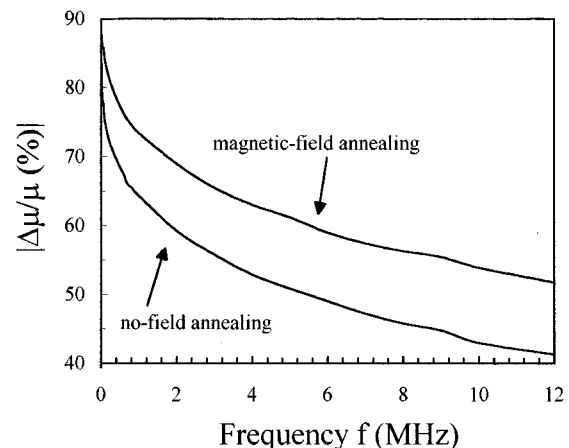


FIG. 4. Frequency dependence of  $\Delta\mu/\mu_{(H_{ex}=0)}$  ( $\Delta\mu = \mu_{(H_{ex})} - \mu_{(H_{ex}=0)}$ ) in transverse- and zero-field annealed states, respectively.

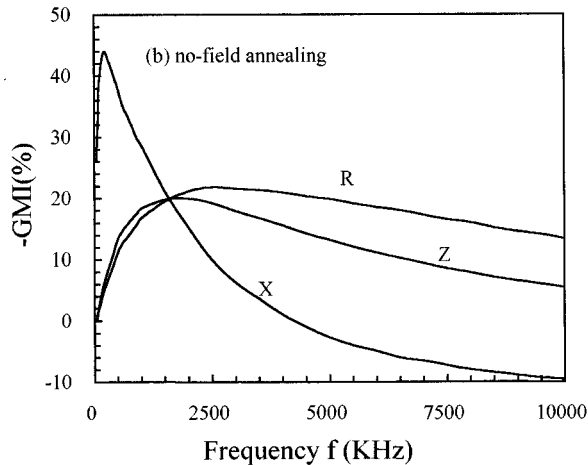
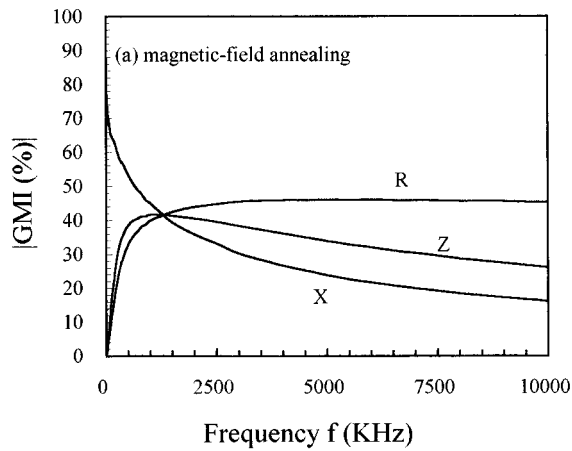


FIG. 5. Frequency dependence of GMI ( $R, X, Z$ ) with the external magnetic field fixed at 5.57 KA/m in (a) field- and (b) nonfield annealed state.

direction of  $H_{ex}$ , then the moment rotation dominated in both the field and nonfield annealed states, this led to the relaxation frequencies moving to higher values. Because the easy magnetization direction was along  $H_{ex}$ , with the application of the same  $H_{ex}$ , the change of the permeability in the field annealed state would be larger than that in the nonfield annealed state.

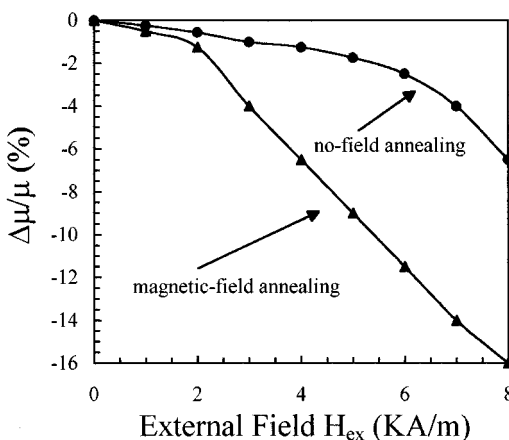


FIG. 6. Field dependence of  $\Delta\mu/\mu_{(H_{ex}=0)}$  in the field and nonfield annealed states.

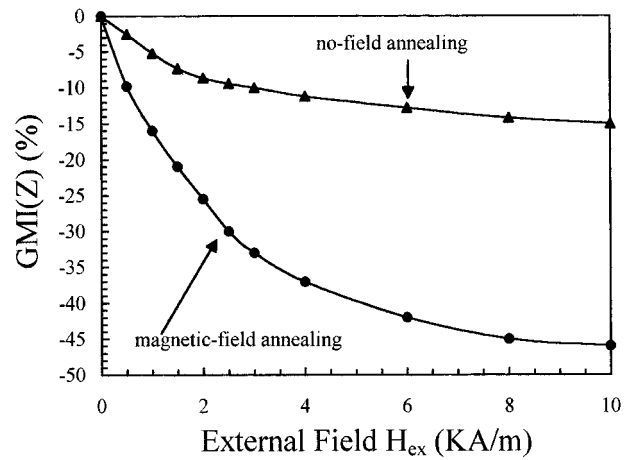


FIG. 7. Field dependence of GMI( $Z$ ) in the field and nonfield annealed states.

With  $H_{ex}$  fixed at 7.57 KA/m, the frequency dependence of GMI( $R, X, Z$ ) is shown in Figs. 5(a) and 5(b). It is obvious that, in the whole frequency range, GMI( $R, X, Z$ ) in the field annealed state was larger than that in the nonfield annealed state, and the former showed its maximum value of 41% at about 1.2 MHz while the latter showed its maximum value of 20% at about 1.6 MHz. According to the origin of GMI effects, in the field annealed state, it was the significant change of permeability that led to the enhancement of the maximum GMI( $Z$ ).

With the ac current frequency fixed at 0.5 MHz, Fig. 6 shows the field dependence of  $\Delta\mu/\mu_{(H_{ex}=0)}$  while Fig. 7 shows the dependence of GMI( $Z$ ). It can be seen from Fig. 6 that  $\Delta\mu/\mu_{(H_{ex}=0)}$  in the field annealed state increased more rapidly with  $H_{ex}$  than that in the nonfield annealed state. It is also obvious that both the magnitudes of  $\Delta\mu/\mu_{(H_{ex}=0)}$  and GMI( $Z$ ) in the former state were larger than that in the latter. These results indicated that  $H_{ex}$  could change the distribution of magnetic domains more effectively in the field annealed state. The reason is that, under this condition, the easy magnetization direction induced by field annealing was parallel to  $H_{ex}$ .

#### IV. CONCLUSION

Magnetic field annealing of  $Fe_{73.5}Cu_1Mo_3Si_{13.5}B_9$  alloy ribbons can result in the easy magnetization direction along  $I_{ac}$  as well as  $H_{ex}$ . This leads to a significant change in the permeability with the application of a smaller  $H_{ex}$ , consequently the GMI effects were enhanced. With the application of the same  $H_{ex}$ , GMI( $Z$ ) values of 41% and 20% have been obtained in  $Fe_{73.5}Cu_1Mo_3Si_{13.5}B_9$  alloy ribbons with transverse field and nonfield annealing, respectively.

#### ACKNOWLEDGMENTS

This work was supported by Foundation of Ministry of Metallurgical Industry and National Nature Science Foundation of China. The authors thank Professor Dan Wei in Tsinghua University for her help.

- <sup>1</sup>K. Mandal and S. K. Ghatak, *Phys. Rev. B* **47**, 14 233 (1993).
- <sup>2</sup>K. Mohri, T. Kohzawa, K. Kawashima, H. Yoshida, and L. V. Panina, *IEEE Trans. Magn.* **28**, 3150 (1992).
- <sup>3</sup>J. Velazquez, M. Vazquez, D.-X. Chen, and A. Hernando, *Phys. Rev. B* **50**, 16 737 (1994).
- <sup>4</sup>R. S. Beach and A. E. Berkowitz, *Appl. Phys. Lett.* **64**, 3652 (1994).
- <sup>5</sup>R. L. Sommer and C. C. Chien, *Appl. Phys. Lett.* **67**, 3346 (1995).
- <sup>6</sup>M. Knobel, M. L. Sanchez, C. Gomez-Polo, P. Marin, M. Vazquez, and A. Hernando, *J. Appl. Phys.* **79**, 1646 (1996).
- <sup>7</sup>Y. Yoshizawa, S. Oguma, and K. Yamauchi, *J. Appl. Phys.* **64**, 6044 (1988).
- <sup>8</sup>L. V. Panina, K. Mohri, T. Uchiyama, and M. Noda, *IEEE Trans. Magn.* **31**, 1249 (1995).
- <sup>9</sup>L. Tao, X. Zu-Xiong, M. Ru-Zhang, J. Song, and Y. Guo-Bin, *Acta Phys. Sin.* **45**, 528 (1996) (in Chinese).
- <sup>10</sup>K. Wanjun, G. Fuding, Y. Ge, and Z. Jing, *Chin. Phys. Lett.* **14**, 310 (1997).
- <sup>11</sup>R. S. Beach, N. Smith, C. L. Platt, F. Jeffers, and A. E. Berkowitz, *Appl. Phys. Lett.* **68**, 2753 (1996).
- <sup>12</sup>K. V. Rao, F. B. Humphrey, and J. L. Costa-Kramer, *J. Appl. Phys.* **76**, 6204 (1994).
- <sup>13</sup>R. L. Sommer and C. L. Chien, *Appl. Phys. Lett.* **67**, 857 (1995).
- <sup>14</sup>R. L. Sommer and C. L. Chien, *J. Appl. Phys.* **79**, 5139 (1996).
- <sup>15</sup>P. Olureanu, P. Rudkowski, G. Rudkowska, D. Menard, M. Britel, J. F. Currie, J. O. Strom-Olsen, and A. Yelon, *J. Appl. Phys.* **79**, 5136 (1996).